Visual Gene Expression Reveals a cone-to-rod Developmental Progression in Deep-Sea Fishes

Nik Lupše,*[,1] Fabio Cortesi,[2] Marko Freese,[3] Lasse Marohn,[3] Jan-Dag Pohlmann,[3] Klaus Wysujack,[3] Reinhold Hanel,[3] and Zuzana Musilova*[,1]

[1]Department of Zoology, Faculty of Science, Charles University, Prague, Czech Republic

[2]Queensland Brain Institute, The University of Queensland, Brisbane, QLD, Australia

[3]Thünen Institute of Fisheries Ecology, Bremerhaven, Germany

***Corresponding authors**: E-mails: lupsen@natur.cuni.cz; zuzana.musilova@natur.cuni.cz

Associate editor: Belinda Chang

Abstract

Vertebrates use cone cells in the retina for color vision and rod cells to see in dim light. Many deep-sea fishes have adapted to their environment to have only rod cells in the retina, while both rod and cone genes are still preserved in their genomes. As deep-sea fish larvae start their lives in the shallow, and only later submerge to the depth, they have to cope with diverse environmental conditions during ontogeny. Using a comparative transcriptomic approach in 20 deep-sea fish species from eight teleost orders, we report on a developmental cone-to-rod switch. While adults mostly rely on rod opsin (*RH1*) for vision in dim light, larvae almost exclusively express middle-wavelength-sensitive ("green") cone opsins (*RH2*) in their retinas. The phototransduction cascade genes follow a similar ontogenetic pattern of cone—followed by rod-specific gene expression in most species, except for the pearleye and sabretooth (Aulopiformes), in which the cone cascade remains dominant throughout development, casting doubts on the photoreceptor cell identity. By inspecting the whole genomes of five deep-sea species (four of them sequenced within this study: *Idiacanthus fasciola, Chauliodus sloani*; Stomiiformes; *Coccorella atlantica*, and *Scopelarchus michaelsarsi*; Aulopiformes), we found that they possess one or two copies of the rod *RH1* opsin gene, and up to seven copies of the cone *RH2* opsin genes in their genomes, while other cone opsin classes have been mostly lost. Our findings hence provide molecular evidence for a limited opsin gene repertoire in deep-sea fishes and a conserved vertebrate pattern whereby cone photoreceptors develop first and rod photoreceptors are added only at later developmental stages.

Key words: **opsin, evolution, mesopelagic, adaptation, convergence, phototransduction, vision, gene expression, rhodopsin.**

Article

Introduction

Vision is a primary sense used by most vertebrates for navigation, predator avoidance, communication and to find food and shelter. At its initiation, vertebrate vision is enabled by cone (photopic, color vision) and rod (scotopic) photoreceptors in the retina containing a light absorbing pigment that consists of an opsin protein covalently bound to a vitamin-A-derived chromophore (Lamb 2013). The absorbance of photons by the chromophore leads to a conformational change of the opsin protein, which initiates a photoreceptor-specific G-protein-coupled phototransduction cascade, propagating the signal to the brain (Downes and Gautam 1999; Larhammar et al. 2009; Lamb 2019). It is thought that the development of the visual system follows a conserved molecular pattern whereby cone specific genes are activated first before the rod molecular pathway is initiated later during ontogeny (Mears et al. 2001; Shen and Raymond 2004; Sernagor et al. 2006). However, whether this is the case for all vertebrates and especially for those that have retinas that contain only rods as adults, remains unclear.

Changes in the light environment, ecology, and phylogenetic inertia are thought to be primary drivers for visual system diversity in vertebrates (Hunt et al. 2014). For example, most mesopelagic deep-sea fishes (200–1,000 m depth), either living strictly at depth or migrating to the shallows at night, have evolved visual systems that are sensitive to the dominant blue light (~470–490 nm) of their environment (Turner et al. 2009). Furthermore, as the daylight and the bioluminescent light emitted by deep-sea critters are quickly dimmed with depth and distance, deep-sea fish visual systems have evolved peculiar morphologies to maximize photon capture including barrel-eyes, reflective tapeta and the use of rod-dominated and in many cases rod-only retinas that might be stacked into multiple banks (reviewed in de Busserolles et al. (2020)). However, most mesopelagic fishes start their lives in the shallow well-lit epipelagic zone (0–200 m depth) (Moser and Smith 1993; Sassa and Hirota 2013). Consequently, their visual systems must cope with a variety of light intensities and spectra throughout development.

Studies investigating the gene expression in the retina of deep-sea fishes are scarce and usually focus on a selected few species (Zhang et al. 2000; Douglas et al. 2016; de Busserolles et al. 2017; Musilova et al. 2019a; Byun et al. 2020). In adults, species with pure rod retinas tend to only express rod opsin(s) (Douglas et al. 2016; Musilova et al. 2019a), albeit two species of pearlsides (*Maurolicus* spp.) have been found to express cone-specific genes (i.e., cone transduction pathway and opsin genes) inside rod-looking cells (de Busserolles et al. 2017). It remains unknown whether deep-sea fishes that have a low proportion of cone photoreceptors as adults (Munk 1990; Collin et al. 1998; Bozzano et al. 2007; Pointer et al. 2007; Biagioni et al. 2016) also express cone-specific genes at any stages of their lives or whether these fishes rely on the rod machinery alone. To investigate whether the retinal development in deep-sea fishes follows a similar cone-to-rod molecular pathway as found in other vertebrates or whether some species start their lives with the rod pathway activated, we set out to sequence the retinal transcriptomes of 20 deep-sea fish species, including the larval stages in ten species, belonging to eight different teleost orders (Argentiniformes, Aulopiformes, Beryciformes, Myctophiformes, Pempheriformes, Scombriformes, Stomiiformes, and Trachichthyiformes). We further investigated the genomic repertoire in five selected species.

Results and Discussion

Opsin Gene Repertoire in the Genome

In teleost fishes, gene duplications and deletions followed by functional diversification have resulted in extant species having between 1 and 40 visual opsin genes within their genomes (Musilova et al. 2019a, 2021). These genes are defined by their photoreceptor specificity, their phylogeny, and their spectrum of maximal sensitivity (λ_{max}) and fall within five major classes, four cone opsins ("ultraviolet or UV sensitive" *SWS1*: 347–383 nm, "blue" *SWS2*: 397–482 nm, "green" *RH2*: 452–537 nm, and "red" *LWS*: 501–573 nm) and one rod opsin ("blue-green" rhodopsin, *RH1* or Rho: 447–525 nm) (Carleton et al. 2020). We analyzed the whole genomes of five deep-sea species (sawtail fish *Idiacanthus fasciola*, viperfish *Chauliodus sloani*; both Stomiiformes; sabretooth *Coccorella atlantica*, pearleye *Scopelarchus michaelsarsi*; both Aulopiformes; and fangtooth *Anoplogaster cornuta*; Trachichthyiformes), four of them sequenced for the purpose of this study. All species possess one or two copies of the rod opsin *RH1* gene, and one to seven copies of the *RH2* cone opsin (fig. 1). All other cone opsin classes, that is, the *SWS1*, *SWS2* (except for the fangtooth) and *LWS* are missing and have been putatively lost during evolution in these five species. This is in accordance with the observation that the *LWS* gene abundance decreases with the habitat depth (Musilova et al. 2019a). Such a limited genomic repertoire most likely represents an evolutionary response to the deep-sea scotopic environment where the shortest (UV-violet) and longest (red) wavelengths of light are filtered out first in the water column, as opposed to middle-range wavelengths that can penetrate to greater depths (reviewed in Musilova et al. 2021; de Busserolles et al. 2020; Carleton et al. 2020). The increased *RH2* diversity observed in the two aulopiform species, on the other hand, illustrates the versatility of this cone opsin class and confirms its dominance in various dimmer-light habitats (Musilova and Cortesi 2021). Here, we confirm that *RH2* is undoubtedly the most important (and often the only) cone opsin gene present in deep-sea fish genomes.

Visual Opsin Gene Expression

Transcriptomic sequencing of 20 deep-sea teleost species revealed that deep-sea fishes mainly express rod opsins and/or green-sensitive cone opsins (*RH2*s) in their retinas (fig. 1 and table 1). While larvae mostly expressed *RH2*, adults and juveniles mostly expressed *RH1* and in a few cases a combination of both. We found none or very low expression of any of the other cone opsin genes: the red sensitive *LWS* was not expressed at all, the UV sensitive *SWS1* was only found in the larva of the whalefish, *Gyrinomimus* sp. (Beryciformes), and the blue/violet sensitive *SWS2* only in the larvae of the whalefish, and the fangtooth, *A. cornuta* (Trachichthyiformes) (fig. 1 and table 1). Differences in gene expression patterns are likely to be driven by ontogenetic transitions in light habitat from bright to dim environments and by changes in ecological demands, as discussed in more detail below.

Similar to the opsin genes, we also detected ontogenetic differences in the expression of phototransduction cascade genes (fig. 2). Here, we focused on the comparison of five species from three teleost orders for which we had both larval and adult specimens available and found that the cone-specific genes were mostly expressed in the larval stages (e.g., cone transducin, *GNAT2*), while adults from three species mostly expressed rod-specific genes (e.g., rod transducin, *GNAT1*; fig. 2*B*). Hence, at the molecular level, the visual systems of deep-sea fishes start out with a cone-based expression pattern. Furthermore, in the fangtooth, where samples from various sized specimens were available, we found that the cone-specific expression was gradually replaced with the rod profile as the fish grew (fig. 2*C* and table S1). This sequence is similar to the visual development in shallower living fishes (e.g., Atlantic cod (Valen et al. 2016), zebrafish (Sernagor et al. 2006)) and terrestrial vertebrates (e.g., mice (Mears et al. 2001), rhesus monkey (La Vail et al. 1991)), where cone photoreceptors are first to develop, followed by temporally and spatially distinct rods (Raymond 1995; Shen and Raymond 2004). The cone-to-rod developmental sequence is therefore likely to be shared across vertebrates, even in species that have pure rod retinas as adults.

Ontogenetic Shift in Expression Profiles and the Transition Phase

The observed developmental changes in the visual system are best explained by the different habitats larval and adult deep-sea fishes inhabit. In general, deep-sea fish larvae live in the shallow epipelagic zone (Moser and Smith 1993) where ambient light levels are sufficiently high to warrant a cone-based visual system. After metamorphosis, deep-sea fishes start to

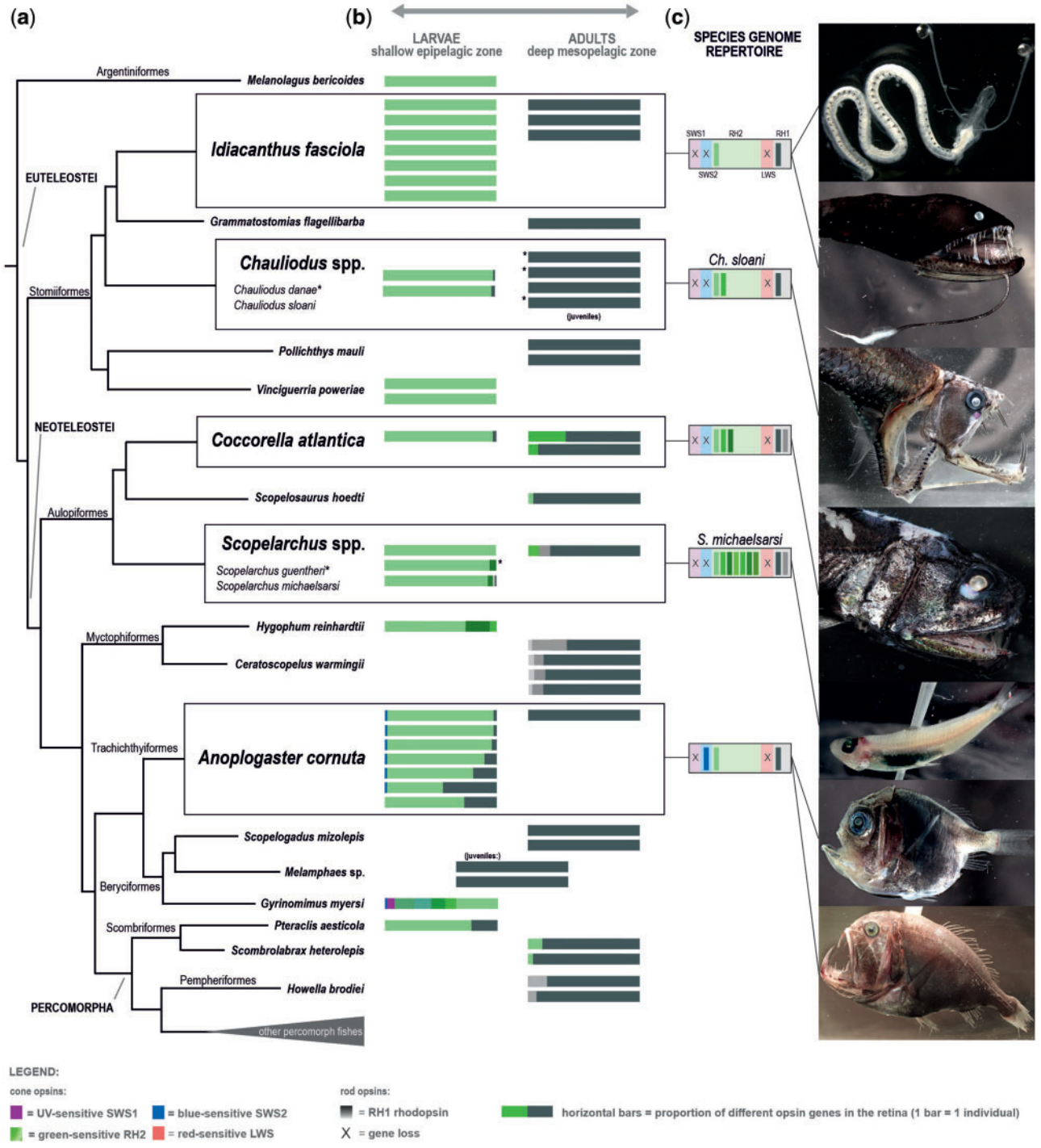

FIG. 1. Cone and rod opsin gene expression in larval and adult deep-sea fishes. (*A*) Simplified phylogeny of the 20 deep-sea fish species for which the retinal transcriptomes were sequenced (topology after Betancur et al. 2017). Boxes highlight the five species for which both larval and adult samples were available. (*B*) Proportional opsin gene expression for each individual (horizontal bars) at different developmental stages. Different colors correspond to cone (colors) or rod (shades of grey) opsin genes, depicted as the proportional expression over the total sum of visual opsins expressed. Different shades of the same color represent multiple copies of the same gene class. Based on the opsin gene expression, the larvae (left column) show a pure-cone or cone-dominated retina, while the adults (right column) have a pure-rod or rod-dominated visual system. Juvenile specimens in two species had an adult expression profile. Note that some species expressed multiple *RH1* copies (*Scopelarchus*, *Howella brodiei*, and *Ceratoscopelus warmingii* adults) or multiple *RH2* copies (*Gyrinomimus* sp. larva, *Hygophum reinhardtii* larva). Notably, adults and larvae of *Scopelarchus* sp. and *Coccorella atlantica* expressed different copies of *RH2* (more details in fig. 2). Details about the samples and expression levels are listed in table 1. (*C*) The genomic repertoire of the visual opsins is shown for five species: *Idiacanthus fasciola*, *Chauliodus sloani*, *Coccorella atlantica*, *Scopelarchus michaelsarsi* (all this study), and *Anoplogaster cornuta* (Musilova et al. 2019a). The rod *RH1* opsin and the cone *RH2* opsin genes are present in all studied species in one or multiple (up to seven) copies. The *SWS2* opsin gene was found only in the fangtooth, and the *SWS1* and *LWS* are missing from all five studied genomes.

Table 1. Samples Used in the Study and Results of the Opsin Gene Expression in the Eyes or Retina.

Species	Order	Median Species Depth (m)[a]	Stage	Code	Size (mm)	Date of Collection	Raw Reads	Reads After Bacteria Filtering	Gene Expression				Accession No.	Source
									RH1	*RH2*	*SWS1*	*SWS2*		
Anoplogaster cornuta	Trachichthyiformes	1000–2000	Larva	39016	4	April 2015	36,373,372	36,125,630	<0.01	0.99		<0.01	SAMN10473242	GenBank
			Larva	39017	4	April 2015	34,712,538	34,604,364	<0.01	0.99		<0.01	SAMN10473243	GenBank
			Larva	4_23	9	April 2015	41,592,840	41,519,070	0.02	0.98		<0.01	SAMN10473246	GenBank
			Larva	4_22	11	April 2015	75,109,270	74,990,214	0.11	0.89		<0.01	SAMN10473245	GenBank
			Larva	4_21	11-12	April 2015	28,945,804	28,869,552	0.22	0.78		<0.01	SAMN10473244	GenBank
			Larva	261s03	12	30.3.2017	48,458,044	48,457,472	0.47	0.53		<0.01	SAMN20741930	This study
			Larva	126A1	20	1.3.2020	79,371,594	79,347,702	0.28	0.72			SAMN20746021	This study
			Adult	56H6	102	6.-7.4.2017	11,658,040	11,635,610	1				SAMN20748547	This study
Ceratoscopelus warmingii	Myctophiformes	400–500	Adult	300s03	63	7.-8.4.2017	49,078,974	44,114,639	0.66 RH1-1 0.01 RH1-2 0.33 RH1-3				SAMN20752508	This study
			Adult	S1	n/a	June 2014	8,796,786	8,789,961	0.94 RH1-1 0.02 RH1-2 0.04 RH1-3				SAMN10473255	GenBank
			Adult	S2	n/a	June 2014	8,655,248	8,649,342	0.93 RH1-1 0.02 RH1-2 0.05 RH1-3				SAMN10473256	GenBank
			Adult	S3	n/a	June 2014	7,904,714	7,899,617	0.94 RH1-1 0.01 RH1-2 0.05 RH1-3				SAMN10473257	GenBank
Chauliodus sloani	Stomiiformes	800–900	Larva	67I2_2	11	3.4.2017	34,445,252	34,371,394	0.01	0.99			SAMN20769443	This study
			Larva	67I1	17	3.4.2017	20,701,686	20,683,764	<0.01	0.99			SAMN20769824	This study
			Juvenile	109B6	20	5.4.2017	24,854,866	24,835,646	1				SAMN20771653	This study
Chauliodus danae	Stomiiformes	800–900	Juvenile	109C7	24	30.3.2017	32,865,334	32,834,300	1				SAMN20771814	This study
			Juvenile	109A2	20	5.4.2017	25,389,318	25,344,182	1				SAMN20777471	This study
			Juvenile	109D7	96	30.3.2017	18,540,248	18,533,484	1				SAMN20777490	This study
Coccorella atlantica	Aulopiformes	300–400	Larva	109G8	21	30.3.2017	26,376,620	26,359,060	0.01	0.99 RH2-1			SAMN20793157	This study
			Adult	56C7	77	25.3.2017	36,794,070	36,790,854	0.69	0.31 RH2-2			SAMN20793158	This study
			Adult	297_7	68	6.-7.4.2017	43,948,534	40,511,279	0.96	0.04 RH2-2			SAMN20793260	This study
Grammatostomias flagellibarba	Stomiiformes	500–600	Adult	56H8	138	6.-7.4.2017	9,775,520	9,742,864	1				SAMN20794729	This study
Gyrinomimus myersi	Beryciformes	1000–2000	Larva	S25	n/a	April 2015	19,270,096	19,122,986	<0.01	0.45 RH2-1 0.13 RH2-2 0.08 RH2-3 0.11 RH2-4 0.15 RH2-5	0.07	<0.01	SAMN10473271	GenBank
Howella brodiei	Pempheriformes	500–600	Adult	56D8	76	25.3.2017	56,905,264	43,936,178	0.17 RH1-1 0.83 RH1-2				SAMN20797093	This study
			Adult	56D9	68	25.3.2017	61,909,674	61,590,270	0.07 RH1-1 0.93 RH1-2				SAMN20799523	This study
Hygophum reinhardtii	Myctophiformes	100–200	Larva	67I2_1	5	3.4.2017	17,222,626	17,122,880		0.26 RH2-1 0.68 RH2-2 0.06 RH2-3			SAMN20799641	This study
Idiacanthus fasciola	Stomiiformes	600–700	Larva	71C2	22	22.3.2017	23,382,468	23,379,360		1			SAMN20800764	This study
			Larva	67D2	22	31.3.2017	6,647,384	6,623,496		1			SAMN20800770	This study
			Larva	71C1	18	22.3.2017	23,632,774	23,497,715		1			SAMN20800774	This study
			Larva	67I7	25	5.4.2017	25,713,960	25,701,768		1			SAMN20800775	This study
			Larva	71B9	14	22.3.2017	43,695,620	43,633,424		1			SAMN20801851	This study
			Larva	67B8	17	29.3.2017	28,333,642	28,313,024		1			SAMN20804813	This study
			Larva	109A1	41	5.4.2017	27,834,274	27,818,750		1			SAMN20804946	This study
			Adult	228s01	210	22.-23.3.2017	21,704,528	21,622,274	1				SAMN20805116	This study
			Adult	67F8	178	1.4.2017	15,744,604	15,739,004	1				SAMN20805515	This study
			Adult	67B6	75	29.3.2017	15,439,954	11,368,044	1				SAMN20834669	This study
Melamphaes sp.	Beryciformes	600–700	Juvenile	4_26	n/a	April 2015	38,583,370	38,534,507	1				SAMN10473273	GenBank
			Juvenile	4_28	n/a	April 2015	35,489,970	35,431,421	1				SAMN10473274	GenBank

(continued)

Table 1. Continued

Species	Order	Median Species Depth (m)[a]	Stage	Code	Size (mm)	Date of Collection	Raw Reads	Reads After Bacteria Filtering	Gene Expression				Accession No.	Source
									RH1	*RH2*	*SWS1*	*SWS2*		
Melanolagus bericoides	Argentiniformes	800–900	Larva	71H3	7	26.3.2017	26,219,646	26,210,402		1			SAMN20834672	This study
Pteraclis aesticola	Scombriformes	0–300	Larva	109H4	8	30.3.2017	19,918,922	19,870,484	0.22	0.78			SAMN20844147	This study
Pollichthys mauli	Stomiiformes	300–400	Adult	109I2	34	30.3.2017	55,767,498	54,875,747	1				SAMN20845044	This study
			Adult	109I3	36	30.3.2017	68,655,686	67,082,709	1				SAMN20848441	This study
Scombrolabrax heterolepis	Scombriformes	800–900	Adult	,56E3	91	25.3.2017	65,770,014	65,527,135	0.98	0.02			SAMN20857047	This study
			Adult	,56E4	77	25.3.2017	60,643,652	60,472,479	0.93	0.07			SAMN20857932	This study
Scopelarchus guentheri	Aulopiformes	200–300	Larva	109H1	21	30.3.2017	37,542,802	37,416,486		0.96^{RH2_larval} $0.04^{RH2\text{-}2\_larval}$			SAMN20859427	This study
Scopelarchus michaelsarsi	Aulopiformes	300–400	Larva	109B9	21	5.4.2017	9,971,250	9,919,148		1^{RH2_larval}			SAMN20860823	This study
			Larva	71B7	20	22.3.2017	43,695,620	43,682,534	$<0.01^{RH1a}$ $<0.01^{RH1b}$	0.96^{RH2_larval} $0.03^{RH2\text{-}2\_larval}$			SAMN20865446	This study
			Adult	272_10	66	2.4.2017	45,565,202	43,729,338	0.80^{RH1a} 0.10^{RH1b}	0.10^{RH2_adult}			SAMN20867027	This study
Scopelogadus mizolepis	Beryciformes	800–900	Adult	,57E2	43	5.4.2017	5,160,876	5,160,672	1				SAMN20867114	This study
			Adult	300s01	62	7.-8.4.2017	15,448,240	15,420,650	1				SAMN20867573	This study
Scopelosaurus hoedti	Aulopiformes	500–600	Adult	297_9	69	6.-7.4.2017	43,948,534	42,248,053	0.98	0.02			SAMN20872996	This study
Vinciguerria poweriae	Stomiiformes	100–300	Larva	109H2	18	30.3.2017	25,863,628	25,755,100		1			SAMN20878005	This study
			Larva	109C8	16	30.3.2017	22,914,004	22,858,398		1			SAMN20882114	This study

[a]https://obis.org/.

submerge deeper and take up a life at different depths in the mesopelagic or even bathypelagic (below 1,000 m depth) zone, where the sun- and moonlight is gradually replaced by bioluminescence as the main source of light (Denton 1990). In this extremely dim environment, rods work at their best and cone photoreceptors would be obsolete for the most part at least. Rod-based vision is also favored in those deep-sea species that exhibit diel vertical migrations to feed in the plankton rich surface layers at night (de Busserolles et al. 2020). In addition, we discovered that in some species there was a switch in the expressed type of cone *RH2* opsin (fig. 1). For example, in Aulopiformes, the larvae expressed an alternative *RH2* copy that is presumably sensitive to longer wavelengths of light compared to the *RH2* that was found in adults (table 2). This clearly shows that larval and adult deep-sea fishes rely on different opsin expression profiles, which is similar to ontogenetic changes in opsin gene expression in diurnal shallow-water fishes such as freshwater cichlids (Carleton et al. 2016) and coral reef dottybacks (Cortesi et al. 2015, 2016) or between the freshwater and deep-sea maturation stages in eels (Zhang et al. 2000).

Our data furthermore suggest that the ontogenetic change in visual gene expression precedes morphological changes such as metamorphosis from larva to juvenile and also habitat transitions. For example, in the fangtooth, the larvae which were collected from the shallows (0–300 m) showed increasing amounts of *RH1* expression with growth, despite displaying larval phenotypes throughout (horns and small teeth; fig. 1). A similar pattern of changing opsin gene expression ahead of metamorphosis has also been reported from shallow-water fishes such as European eels (Bowmaker et al. 2008), dottybacks (Cortesi et al. 2016), and surgeonfishes (Tettamanti et al. 2019). Interestingly, all our fangtooth larvae (including the smallest individual with a total length of 4 mm) already expressed a small amount of *RH1* (fig. 2C). Whether fangtooth start their lives with a pure cone retina or low-levels of rod opsin expression are normal even in preflexation larvae remains therefore unclear. In addition to the green-sensitive cone opsin *RH2*, the smallest fangtooth larvae also expressed low levels of the blue-sensitive *SWS2*, potentially conferring dichromatic color vision to the early-life stages of this species (fig. 1).

Photoreceptor Cell Identities

Interestingly, two aulopiform species, the Atlantic sabretooth, *C. atlantica*, and the Bigfin pearleye, *S. michaelsarsi*, despite expressing mostly *RH1* as adults, retained a cone-dominated phototransduction cascade expression profile akin to the one found in the larval stages (fig. 2 and table S1). This begs the question whether the photoreceptors they are using are cones or rods in nature. Initially described in snakes and geckos (Simoes et al. 2016; Schott et al. 2019) and recently also in a deep-sea fish (de Busserolles et al. 2017), it appears that the dichotomy of rods and cones is not always as clear cut as one might think. For example, adult deep-sea pearlsides, *Maurolicus* spp. have a retina that expresses ~99% *RH2* and ~1% *RH1* with corresponding cone and rod phototransduction gene expressions. Their photoreceptors, however, are all rod-shaped and careful histological examination has

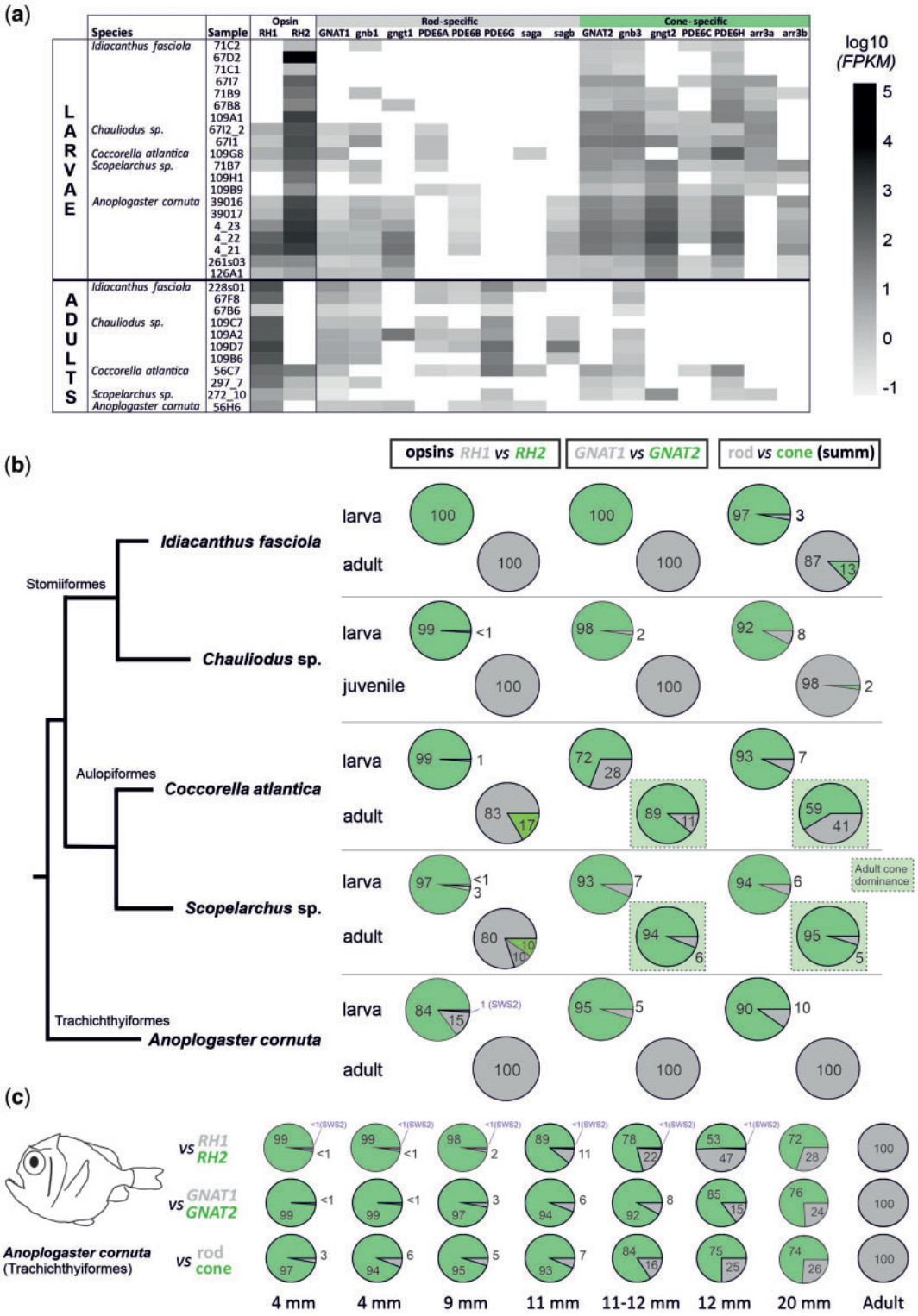

FIG. 2. Phototransduction cascade gene expression in the retina of five deep-sea fish species. (*A*) Heat map of the expression of individual phototransduction cascade genes for each sample, based on normalized numbers of reads (FPKM). (*B*) Pie charts comparing mean values of relative expression of the opsin genes (rod *RH1* and cone *RH2*), photoreceptor-specific cascade transducin genes (rod-type *GNAT1* and cone-type *GNAT2*), and all cascade genes excluding opsins (photoreceptor-specific transducins, arrestins and phosphodiesterases) summarized. The green rectangles highlight the two aulopiform species with the discordance between the opsin type (rod-specific) and phototransduction cascade genes (cone-specific) in adults. (*C*) Focus on the common fangtooth (*Anoplogaster cornuta*) transitional phase shown as a sequence for seven larval and one adult sample. Size given as standard length (SL). Note that all fangtooth larvae expressed both *RH1 and RH2*, with an increasing proportion of *RH1* to *RH2* as the larvae grew in size (with the exception of the largest larva where *RH1:RH2* was 28:72). Smaller larvae also expressed the *SWS2* gene. Except for the adult, all other individuals had traits of larval phenotypes (dorsal and ventral horns and small teeth; fig. 1) and were collected relatively shallow between 0 and 300 m using plankton trawls.

Table 2. Key-Tuning Amino Acid Sites in the Cone Opsin *RH2* Gene.

Species	Order	83	122	207	255	292	λ_{max} (nm)	Reference
Bovine RH1		**D**	**E**	**M**	**I**	**A**	**500**	**Yokoyama (2008)**
Ancestral teleost		**D**	**Q**	**M**	**I**	**A**	**488**	**Yokoyama and Jia (2020)**
Melanolagus bericoides	**Argentiniformes**	G	Q	.	V	.		
***Coccorella atlantica* adult**	**Aulopiformes**	G	Q	.	.	.		
***Coccorella atlantica* larval**	**Aulopiformes**	G	Q	.	V	.		
***Scopelarchus michaelsarsi*_ RH2_adult**	**Aulopiformes**	?	Q	I	C	T		
***Scopelarchus guentheri* _RH2_larval**	**Aulopiformes**	G	Q	.	V	.		
***Scopelarchus michaelsarsi*_ RH2_ larval**	**Aulopiformes**	G	Q	.	V	.	505	**Pointer et al. (2007) (for *S. analis*)**
***Scopelarchus guentheri*_ RH2-2_ larval**	**Aulopiformes**	G	Q	.	C	.		
***Scopelarchus michaelsarsi*_ RH2-2_ larval**	**Aulopiformes**	G	Q	.	C	.		
Scopelosaurus hoedti	**Aulopiformes**	G	Q	.	.	.		
***Gyrinomimus myersi* RH2-1**	**Beryciformes**	G	Q	.	F	.		
***Gyrinomimus myersi* RH2-2**	**Beryciformes**	G	Q	L	F	.		
***Gyrinomimus myersi* RH2-3**	**Beryciformes**	G	Q	L	F	.		
***Gyrinomimus myersi* RH2-4**	**Beryciformes**	G	Q	L	F	.		
***Gyrinomimus myersi* RH2-5**	**Beryciformes**	G	Q	L	F	.		
***Lepisosteus platyrhincus* (shallow outgroup)**	**Lepisosteiformes**	G	.	.	.	.		
***Hygophum reinhardtii* RH2-1**	**Myctophiformes**	G	Q	.	V	.		
***Hygophum reinhardtii* RH2-2**	**Myctophiformes**	G	Q	.	V	.		
***Hygophum reinhardtii* RH2-3**	**Myctophiformes**	G	Q	.	V	.		
***Lepidopus fitchi* RH2-1**	**Scombriformes**	G	.	.	V	.	496	**Yokoyama and Jia (2020)**
***Lepidopus fitchi* RH2-2**	**Scombriformes**	G	Q	.	V	.		
***Lepidopus fitchi* RH2-3**	**Scombriformes**	G	Q	.	V	.	506	**Yokoyama and Jia (2020)**
***Lepidopus fitchi* RH2-4**	**Scombriformes**	G	Q	.	V	.		
Pteraclis aesticola	**Scombriformes**	G	Q	L	.	.		
Scombrolabrax heterolepis	**Scombriformes**	G	Q	.	.	.		
Aristostomias scintillans	**Stomiiformes**	G	Q	L	V	.	468	**Yokoyama and Jia (2020)**
***Chauliodus* sp.**	**Stomiiformes**	G	Q	.	F	.		
Grammatostomias flagellibarba	**Stomiiformes**	G	Q	.	.	.		
Idiacanthus fasciola	**Stomiiformes**	G	Q	.	V	.		
Vinciguerria poweriae	**Stomiiformes**	G	Q	.	F	.		
Anoplogaster cornuta	**Trachichthyiformes**	G	Q	.	.	.		

shown that these consist of a tiny proportion of true rods and a majority of transmuted rod-like cones (de Busserolles et al. 2017). In the case of pearlsides, and also in geckos and snakes, the opsin and phototransduction genes correspond to each other making it possible to distinguish photoreceptor types at the molecular level. However, in the aulopiforms, high expression of rod opsin is seemingly mismatched with high levels of cone phototransduction gene expression (fig. 2). In salamanders, the opposite pattern can be found whereby a cone opsin is combined with the rod phototransduction cascade inside a rod looking cone photoreceptor (Mariani 1986). Anatomically, the retina of *S. michaelsarsi* is composed of mostly rods with low numbers of cone cells (Collin et al. 1998), while the adult retina of *Evermanella balbo*, an evermannellid species related to *C. atlantica*, appears to consist of two differently looking rod populations (Wagner et al. 2019). It is therefore likely, as found in pearlsides (de Busserolles et al. 2017), that these fishes have a high proportion of transmuted rod-like cone photoreceptors, but that they use *RH1* instead of a cone opsin as the visual pigment. Alternatively, a proportion of true rods might make use of the cone phototransduction cascade. Either way, combining more stable rod opsin in a rod-shaped cell with the cone-specific cascade is likely to increase sensitivity while also maintaining high transduction and recovery speeds of cells (Baylor 1987, Kawamura and Tachibanaki 2012, Luo et al. 2020). Histology, fluorescent in situ hybridization and ideally physiological recordings are needed to ultimately disentangle the identity of photoreceptor cells in aulopiforms.

Evolutionary History of Deep-Sea Fish Opsins

While the majority of adult fishes relied on a single *RH1* copy, we found three species that expressed multiple *RH1* copies: The Warming's lanternfish, *Ceratoscopelus warmingii* (Myctophiformes), expressed three different *RH1* genes, and *S. michaelsarsi* and the basslet, *Howella brodiei* (Pempheriformes), expressed two copies each. Larvae and a few adult deep-sea fishes mostly expressed a single *RH2* copy, except for the pearleyes, *Scopelarchus* spp., and the Reinhardt's lanternfish, *Hygophum reinhardtii*, which expressed up to three larval copies each, and the whalefish (*Gyrinomimus* sp.) which expressed five larval copies (fig. 1).

The *RH1 and RH2* phylogenies revealed that most deep-sea fish visual opsins cluster together by species or order (fig. 3). For example, in the whalefish all *RH2s* are clustered together suggesting that these genes are lineage or species-specific duplicates (fig. 3*B*). However, there were a few exceptions, suggesting more ancient duplication events. In *Scopelarchus* the two *RH1* copies are not in a sister relationship and in fact result in different clusters, suggesting that these copies originated in the common ancestor of aulopiforms or perhaps even earlier (fig. 3*A*). Similarly, the *RH2s* in aulopiforms (*Scopelarchus*, *Coccorella*) cluster by ontogenetic stage, making it likely that the

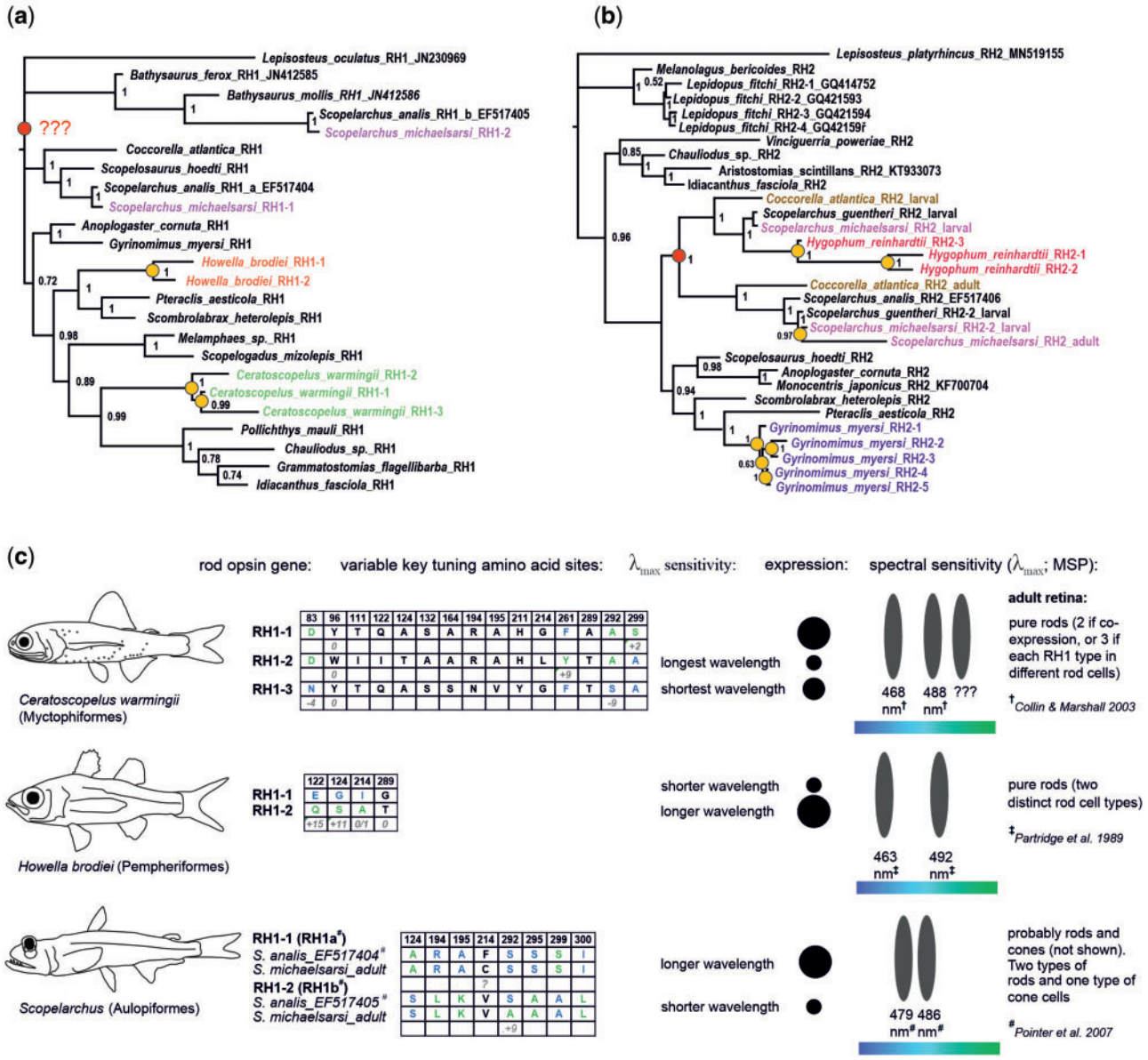

FIG. 3. Gene trees of the (*A*) *RH1* and (*B*) *RH2* opsin genes found in the retinal transcriptomes of deep-sea fishes. Species with multiple copies are highlighted in color. Additional gene sequences from public databases are listed with their GenBank accession numbers. Note the topology within Aulopiformes; the adult *RH2s* of *Cocorrella atlantica and Scopelarchus* cluster together as do the major larval *RH2s*. Yellow circles mark lineage-specific gene duplication events, while red circles pinpoint the ancestral duplication of *RH1* impacting the *Scopelarchus* genus, and the duplication of *RH2* in the aulopiform ancestor (or at least the common ancestor of *Coccorella and Scopelarchus*). (*C*) Key tuning spectral site mutations in species with multiple rod opsins and indicative wavelength shifts based on previous in vitro experiments. Known shifts are listed in nanometers if available. Blue and green letters in the tables stand for the shorter- and longer-shifting amino acid variants, respectively. Multiple different rod opsins have been found in three species, *Ceratoscopelus warmingii* (Myctophiformes), *Howella brodiei* (Pempheriformes), and *Scopelarchus michaelsarsi* (Aulopiformes). Note that the *RH1* copies in *Scopelarchus* seem to show a mixed pattern—the longer-wavelength sensitive copy (*RH1a*; confirmed by in vitro measurements by Pointer et al. (2007) carries also several shorter-shifting amino-acid sites as compared to *RH1b*). Assignment of the longer and shorter wavelength sensitive photoreceptor to a rhodopsin sequence is marked next to the tables. Rhodopsin gene expression marks dominant (large circles) and less abundant (small circles) copies. For functional interpretation of the rod cells in the visual system we considered microspectrophotometry measurements from # = Pointer et al. (2007), † = Collin and Marshall (2003), and ‡ = Partridge et al. (1989).

developmental switch in gene expression was already present in the aulopiform ancestor (fig. 3*B*).

Molecular Complexity of Deep-Sea Fish Visual Systems

The complexity of the deep-sea fish visual systems at the molecular level varied quite substantially. For example, the three Stomiiformes species: The Ribbon sawtail fish, *I. fasciola*, and two species of viperfish, *C. sloani* and *Ch. danae*, appeared to have a very basic visual set up; these fishes were found to express a single *RH2* cone opsin as larvae and a single *RH1* rod opsin as adults (fig. 1). On the contrary, several deep-sea fish orders examined here expressed more than one opsin gene. Adult lanternfishes and basslets have rod-only retinas but

expressed multiple *RH1* copies that have functionally diversified (fig. 3). Other species expressed both cone and rod opsins as adults (the aulopiform species and *Scombrolabrax*), which is somewhat similar to the opsin gene expression profiles found in shallow-living nocturnal reef fishes (Cortesi et al. 2020).

The most complex visual system in this study was found in *S. michaelsarsi*. In general, this species is known for its numerous morphological and anatomical adaptations to vision in the deep, including having barrel eyes with a main and an accessory retina, rods that are organized in bundles, large ganglion cells and corneal lens pads (Collin et al., 1998). The two copies of *RH1* (*RH1a* and *RH1b*) it expressed showed high sequence diversity differing in 79 out of 354 amino acids, eight of which are known key tuning sites likely to change the spectral sensitivity of the pigments via a shift in λ_{max} (fig. 3 and table 3) (Yokoyama 2008; Musilova et al. 2019a; Yokoyama and Jia 2020). This supports the findings by Pointer et al. (2007) who, using in vitro visual pigment expression in another pearleye species, *S. analis*, found two rod photoreceptors with different absorption maxima at 479 and 486 nm. Interestingly, Pointer et al. (2007) also speculate that another short-shifted opsin (previously measured in *S. analis* to have λ_{max} at 444 nm by Partridge et al., 1992) possibly belongs to the *SWS2* class. Our data however does not support this prediction as no SWS2 gene is found in the genome of *S. michaelsarsi*. The existence and identity of such short-sensitive opsins in pearleyes remains therefore elusive. The situation is less clear for the green-sensitive *RH2* opsin. While in *S. analis* cones have been found in the accessory and main retinas, in *S. michaelsarsi* cone photoreceptors appear restricted to the accessory retina alone (Collin et al. 1998). This is intriguing as it suggests substantial differences in visual systems even between closely related species from the same genus.

The Visual Ecology of Deep-Sea Fishes

We found molecular support for deep-sea visual adaptations on multiple levels:

(1) *Opsin gene diversity in the genome.* Data from the genomes of five deep-sea species revealed the diversity of the opsin genes (fig. 1C). Retinal transcriptomes in the Stomiiformes pointed towards a simple visual system that is based on a single expressed opsin gene at different developmental stages (*RH2* in larvae, *RH1* in adults) (fig. 1). A search for visual opsins in the stomiiform genomes sequenced for the purpose of this study (*I. fasciola and Ch. sloani*), as well as in several published genomes (Musilova et al. 2019a) revealed that Stomiiformes are likely to have lost all cone opsin gene classes except for *RH2* (fig. 1). In the case of *RH2*, they seem to only have a single or at most two gene copies, which is substantially less than other teleosts (Musilova et al. 2019a; Musilova and Cortesi, 2021). The stomiiform example, therefore, shows that a decrease in light intensity and the spectrum of light in the deep-sea may not only restrict gene expression at adult stages, but also lead to the loss of opsin genes altogether. Similarly, a loss in opsin and other vision-related genes (e.g., otx5b, crx) has previously been reported from shallow living fishes that are either nocturnal (Luehrmann et al. 2019), live in murky waters (Liu et al. 2019), or inhabit caves or similarly dim environments (Huang et al. 2019; Musilova et al. 2019a). Contrarily, the genomes of two aulopiform species (*C. atlantica and S. michaelsarsi*) revealed expanded cone opsin gene repertoires achieved mostly through *RH2* duplications (*C. atlantica* with three *RH2*s, and *S. michaelsarsi* with seven *RH2* genes; fig 1). Both species also possess two copies of the rod opsin gene. These species inhabit relatively shallower depths (300–400 m) compared to other deep-sea fishes such as the Stomiiformes (table 1). It is likely that having extra copies of *RH2* cone opsins may benefit their vision at these photon-richer depths. It is also possible that an evolutionary stochasticity and the gene content in the ancestor have contributed to the observed pattern. To be able to clearly state this, future research should be done on multiple aulopiform species.

(2) *Visual gene expression.* Previous work has found that the expression of the longest- (*LWS*—red) and shortest- (*SWS1*—UV) sensitive opsins is reduced or absent in deeper living coral reef fishes (Cortesi et al. 2020) and in fishes inhabiting deep freshwater lakes (Hunt et al. 1997; Sugawara et al. 2005; Musilova et al. 2019b), which is correlated with a loss of short- and long-wavelengths with depth. Also, many deep-sea fish lineages have lost *LWS* from their genomes (Musilova et al. 2019a; Cortesi et al. 2021). Supporting these findings, we show here that deep-sea fishes lack any *LWS* expression even in the shallow-living larval stages (fig. 1). Similarly, *SWS1* is not expressed in any of the species studied, except for in the larval whalefish, and is also absent from many deep-sea fish genomes (fig. 1) (Musilova et al. 2019a). However, shallow larval stages are likely to explain why all deep-sea fishes studied to date maintain at least some cone opsins in their genomes (Musilova et al. 2019a). Most deep-sea fish larvae expressed a single *RH2* gene, but the larvae of some species (fangtooth, whalefish, and lanternfish) expressed multiple cone opsin genes (fig. 1). This is likely to provide them with similar visual systems to the larvae of shallow-living marine (Britt et al. 2001) and freshwater species (Carleton et al. 2016), possibly aiding in detecting residual light and discriminating brightness and/or colors. Juvenile deep-sea fishes, on the other hand, showed rod-based expression profiles also found in the adult stages (fig. 1). This shift in opsin gene expression correlates with developmental changes in ecology. As opposed to the adults which are exposed to a narrow and dim light environment where food is scarce, larvae typically live in well-lit, broad spectrum shallow waters where food and predators are abundant (Moser and Smith 1993).

(3) *Functional adaptation in key spectral tuning sites.* When multiple *RH1* copies were expressed, they often showed

Table 3. Key-Tuning Amino Acid Sites in the Rhodopsin *RH1* Gene.

Species	Order	83	90	96	102	111	113	118	122	124	132	164	183	188	194	195	207	208	211	214	253	261	265	269	289	292	295	299	300	317	λ_{max} (nm)	References
Bovine RH1		D	G	Y	Y	N	E	T	E	A	A	A	M	G	P	H	M	F	H	I	M	F	W	A	T	A	A	A	V	M	500	Yokoyama (2008)
Ancestral teleost RH1		D	G	Y	Y		E	T	E	A	A	A	M		L	N	M	F	H	I	M	F	W	A	T	A	A	A	L	M		Musilova et al. (2019a)
Bathysaurus ferox	Aulopiformes	N	.	.	.	.	.	.	.	S	.	.	.	.	R	A	.	.	.	.	.	.	.	.	.	S	.	T	L	.	481	Collin and Marshall (2003)
Bathysaurus mollis	Aulopiformes	N	.	.	.	.	.	.	.	S	.	.	.	.	R	A	.	.	.	.	.	.	.	T	.	S	.	T	L	.	479	Collin and Marshall (2003)
Coccorella atlantica	Aulopiformes	N	.	.	.	S	.	.	M	.	.	.	.	.	R	A	.	.	.	C	.	.	.	.	.	.	S	.	I	.	480[c]	Douglas et al. (1998)
Scopelarchus michaelsarsi RH1a	Aulopiformes	N	.	.	.	.	.	.	.	.	.	.	.	.	R	A	.	.	.	C	.	.	.	.	.	S	S	S	I	.	486[a]	Pointer et al. (2007)
Scopelarchus michaelsarsi RH1b	Aulopiformes	N	.	.	.	.	.	.	.	S	.	.	.	.	L	K	.	.	.	V	.	.	.	.	.	.	.	.	L	.	479[a]	Pointer et al. (2007)
Scopelosaurus hoedti	Aulopiformes	.	.	.	.	.	.	.	.	.	.	.	.	.	R	A	.	.	.	.	.	.	.	.	.	S	S	S	I	.		
Gyrinomimus myersi	Beryciformes	N	.	.	.	.	.	.	.	.	.	.	.	.	R	A	.	.	.	.	.	.	.	.	.	S	.	.	I	.		
Melamphaes sp.	Beryciformes	.	.	.	.	.	.	.	Q	.	S	.	.	.	R	V	.	.	.	G	.	.	.	S	.	.	.	S	I	.		
Scopelogadus mizolepis	Beryciformes	.	.	.	.	.	.	.	Q	G	S	.	.	.	R	V	.	.	.	G	.	.	.	T	.	.	.	S	.	.	488[d]	Douglas et al. (1998)
Lepisosteus oculatus (outgroup)	Lepisosteiformes	.	.	.	.	.	.	.	Q	S	.	.	.	.	L	K	.	.	.	L	.	Y	.	G	.	.	.	.	L	.		
Ceratoscopelus warmingii RH1-1	Myctophiformes	.	.	.	.	T	.	.	Q	.	S	.	.	.	R	A	.	.	.	G	.	.	.	.	A	.	.	S	I	.	488[b]	Collin and Marshall (2003)
Ceratoscopelus warmingii RH1-2	Myctophiformes	.	.	W	.	I	.	.	I	T	.	.	.	.	R	A	.	.	.	L	.	Y	.	.	.	.	.	.	I	.	undetected	Collin and Marshall (2003)
Ceratoscopelus warmingii RH1-3	Myctophiformes	N	.	.	.	T	.	.	Q	.	S	S	.	.	N	V	.	.	Y	G	.	.	.	.	.	S	.	.	I	.	468[b]	Collin and Marshall (2003)
Hygophum reinhardtii	Myctophiformes	.	.	.	.	A	.	.	Q	.	.	.	.	.	R	A	.	.	.	G	.	.	.	.	.	.	.	.	I	.		
Howella brodiei RH1-1	Pempheriformes	N	.	.	.	.	.	.	.	G	.	.	.	.	R	A	.	.	.	.	.	.	.	.	G	S	S	S	I	.		
Howella brodiei RH1-2	Pempheriformes	N	.	.	.	.	.	.	Q	S	.	.	.	.	R	A	.	.	.	A	.	.	.	.	.	S	S	S	I	.		
Pteraclis aesticola	Scombriformes	.	.	.	.	.	.	.	Q	.	.	.	.	.	R	A	.	.	.	.	.	.	.	.	.	.	.	S	I	.		
Scombrolabrax heterolepis	Scombriformes	.	.	.	.	.	.	.	Q	.	.	.	.	.	R	A	.	.	.	.	.	.	.	S	.	S	.	S	I	.		
Chauliodus spp.	Stomiiformes	N	.	.	.	.	.	.	.	G	.	.	.	.	R	A	.	.	.	V	.	.	.	.	A	S	.	.	L	V	484	Collin and Marshall (2003)
Grammatostomias flagellibarba	Stomiiformes	N	.	.	.	.	.	.	.	.	.	.	.	.	R	A	.	.	.	V	.	.	.	.	.	S	.	.	L	.	480 - 487	Kenaley et al. (2014)
Idiacanthus fasciola	Stomiiformes	N	.	.	.	.	.	.	.	.	.	.	.	.	R	A	.	.	.	.	.	.	.	.	.	S	.	.	L	.	485	Collin and Marshall (2003)
Pollichthys mauli	Stomiiformes	N	.	.	.	.	.	.	.	.	.	.	.	.	R	A	.	.	.	.	.	.	.	.	.	S	.	.	L	.		
Anoplogaster cornuta	Trachichthyiformes	N	.	.	.	.	.	.	.	.	.	.	.	.	R	A	.	.	.	.	.	.	.	.	T	S	.	S	I	.	485	Collin and Marshall (2003)

[a]Value for *Scopelarchus analis*.

[b]Two pigments reported without assignment to the gene; see also fig. 3.

[c]Value for closely related species, *Evermannella balbo*.

[d]Value for *Scopelogadus beani*.

distinct differences in key amino acid sites that are likely to shift the spectral sensitivities of the pigments (fig. 3 and table 3) (Yokoyama 2008; Musilova et al. 2019a). Estimating spectral absorbance from these sites resulted in very similar λ_{max} values to those that were measured in vivo from the same or closely related species using microspectrophotometry (MSP) or similar techniques (Partridge et al. 1989; Collin and Marshall 2003; Pointer et al. 2007) (fig. 3 and table 3). We therefore integrated the available functional evidence (MSP values) with our molecular data (protein sequence and gene expression levels) to better understand the function of the visual system in the three species that expressed multiple rod opsins (fig. 3 and table 3).

The three different *RH1*s in *C. warmingii* differed in 15 key-tuning sites. Our data revealed a dominant rod opsin copy (*RH1-1*), and a shorter- (*RH1-2*) and a longer-shifted (*RH1-3*) copies with lower transcript levels (figs. 1 and 3). Previously, MSP in *C. warmingii* has revealed two distinct rod types with λ_{max} values of 488 and 468 nm (Collin and Marshall 2003), most likely corresponding to the *RH1a/RH1-1 and RH1b/RH1-3* genes, respectively. It is possible that multiple *RH1* copies are coexpressed within the same photoreceptor, something that has previously been reported for cone opsins in shallow-water marine (Savelli et al. 2018; Stieb et al. 2019) and freshwater fishes (Dalton et al. 2014; Torres-Dowdall et al. 2017). Coexpression could produce visual pigment mixtures that shift photoreceptor sensitivity and enhance visual contrast, aiding in predator–prey interactions or mate detection (Dalton et al. 2014). Alternatively, we predict that a third rod photoreceptor type with longer spectral sensitivity (*RH1-2*; fig 3C) exists, possibly overlooked during MSP, which can happen especially if the cell type is rare. While the function of having multiple rod opsins in *C. warmingii* remains to be investigated, several possible benefits for a multi-rod visual system have recently been proposed including that it might enable conventional or unusual color vision in dim light, it might be used to increase visual sensitivity, or enhance an object's contrast against a certain background (Musilova et al. 2019a).

In *H. brodiei*, the second *RH1* copy (*RH1-2*) differed in two key-tuning sites, E122Q (−15 nm) and G124S (−11 nm), known to cause major short-wavelength shifts in other fishes (Yokoyama 2008). This is in accordance with the MSP measurements in its sister species, *Howella sherborni*, which found two different rod types with spectral sensitivities of 463 and 492 nm (fig. 3) (Partridge et al. 1989). Having multiple differently tuned rod photoreceptors, one centered on the prevailing light (bioluminescence and/or ambient light ∼480–490 nm) and a second one that is offset from it (i.e., the offset pigment hypothesis; Lythgoe 1966), may be beneficial to break counter illumination of prey—a way of active camouflage in mesopelagic organisms where ventral photophores emit bioluminescent light that matches the residual downwelling light (Denton et al. 1985). Hence, revealing an individual's silhouette could help to distinguish prey and predators from the background lighting, or visually finding mates. However, apart from lanternfishes with three (or more) and basslets with two rod opsins, or exceptional cases of tube-eye (6) and spinyfin (38), the majority of the deep-sea fishes seem to have only one rod opsin (Musilova et al., 2019a).

Differences in spectral sensitivity between photoreceptors can also be due to the chromophore type that binds to the opsin protein; visual pigments with a vitamin A1-based chromophore (typical in marine fishes) confer shorter-shifted λ_{max} values compared to those with a vitamin A2-based chromophore (typical in freshwater fishes) (Carleton et al. 2016). *Cyp27c1* is the enzyme responsible for converting A1- to A2-based chromophores (Enright et al. 2015), with high expression levels suggesting the presence of longer-shifted visual pigments. However, *Cyp27c1* was not expressed in our data set suggesting that the visual pigments of these deep-sea fishes are based on A1-retinal alone (table S2).

Conclusions

So far, the development of deep-sea fish vision at the molecular level had not been studied in detail and only limited morphological information is available. In this study, we compared opsin and visual gene expression between 20 deep-sea fish species revealing a major change in expression between larval and adult stages. While deep-sea fish genomes contain both cone and rod opsin genes, larvae rely on the cone pathway and adults switch to a rod-dominated or rod-only visual system. The cone- versus rod-specific phototransduction cascade genes follow the opsins in some lineages, however, not in aulopiforms, suggesting the presence of transmuted photoreceptor cells. We detected reduced opsin gene repertoires in the genomes of five deep-sea fish species composed only of one rod (*RH1*) and one or two cone (*RH2*, or *RH2 and SWS2*) opsin gene classes. Interestingly, we have identified lineage-specific opsin gene duplications, possibly allowing for increased visual sensitivity and/or color vision in the deep in some species. Overall, our molecular results support a conserved developmental progression in vertebrates whereby cones appear first in the retina and rod photoreceptors are added later during development.

Materials and Methods

Specimens used in this study were collected in the Sargasso Sea during three multipurpose fishery surveys conducted by the German Thünen Institute of Fisheries Ecology onboard the research vessels *Maria S. Merian* in March to April 2015, and *Walther Herwig III* in 2017 and in 2020. The sampling of adults occurred during both day and night at depths of 600–1,000 m using a mid-water pelagic trawl net (Engel Netze, Bremerhaven, Germany) with an opening of 30 × 20 m, a length of 145 m, and mesh sizes (knot to knot) from 90 cm decreasing stepwise to 40, 20, 10, 5, 4, 3, 2 cm, with a 1.5-cm mesh in the 27-m-long codend. The larvae were mostly collected using an Isaacs-Kidd Midwater Trawl net (IKMT; 6.2 m^2 mouth-opening, 0.5 mm mesh size; Hydro-Bios Apparatebau

GmbH) at depths of 0–300 m by double-oblique transect tows. Adult fish were flash-frozen at −80°C upon arrival on board and a fin clip was stored in 96% ethanol. Larval samples were fixed in RNAlater™ (ThermoFisher) and stored at −80°C until further use.

To sequence the whole genome of *I. fasciola*, *C. sloani*, *C. atlantica*, and *S. michaelsarsi*, the genomic DNA was extracted from the fin clip using the DNeasy Blood and Tissue kit (Qiagen) following the enclosed protocol. The library preparation and genome sequencing on Illumina NovaSeq platform (150 bp PE and the yield over 20 Gb per genome) has been outsourced to the sequencing center Novogene, Singapore (https://en.novogene.com/). To analyze the opsin gene repertoire, the raw genomic reads were mapped in Geneious software version 11.0.3 (Kearse et al. 2012) against the opsin references (single exons of all five opsin classes from the reference species: Nile tilapia, Round goby, Blind cavefish, and Spotted gar), as well as against the genes found in the transcriptomes of each species. The parameters were set to the medium sensitivity to capture all reads that matched any visual opsin gene. The captured reads mapping to all exons were then remapped against one reference per exon and the species-specific consensus sequence was generated. If present, multiple paralogous genes were disentangled manually, and the consensus sequence was exported for each variant (see below more details for the transcriptomic analysis). The obtained consensus sequences served as references for the second round of mapping, whereby all genomic reads were again mapped with the Low Sensitivity settings, and each reference was then elongated by the overlapping sequence. This step was repeated until the full gene region was covered. In case of *S. michaelsarsi*, we were not able to cover the full length of five out of seven *RH2* genes due to the repetitions and these genes were reported in two parts, always one covering the exons 1 and 2, and one covering exons 3, 4 and 5. The genomic raw reads are available from GenBank (BioProject PRJNA754116) and the opsin gene sequences are provided in Supplementary file 1.

Total RNA was extracted from the whole eyes using either the RNeasy micro or mini kit (Qiagen) and the extracted RNA concentration and integrity were subsequently verified on a 2100 Bioanalyzer (Agilent). RNAseq libraries for 31 samples were constructed in-house from unfragmented total RNA using Illumina's NEBNext Ultra II Directional RNA library preparation kit, NEBNext Multiplex Oligos and the NEBNext Poly(A) mRNA Magnetic Isolation Module (New England Biolabs). Multiplexed libraries were sequenced on the Illumina HiSeq 2500 platform as 150 bp paired-end (PE) reads. Library construction and sequencing (150 bp PE) for an additional 10 samples was outsourced to Novogene, Singapore (https://en.novogene.com/). We additionally reanalyzed 11 retinal transcriptomes previously published in Musilova et al. (2019a). Together, then, our data set comprised 53 samples of which, based on morphology, 26 were classified as larvae, 6 as juveniles and 21 as adults. Sample IDs, number of raw reads, individual accession numbers for BioProject PRJNA754116 and further parameters are listed in table 1. Single genes extracted from the transcriptomic data are available in Supplemetary file 1.

The sequence data was quality-checked using FastQC (Andrews 2017). Opsin gene expression was then quantified using Geneious software version 11.0.3 (Kearse et al. 2012). For each sample we first mapped the reads against a general fish reference data set comprising all visual opsin genes from the Nile tilapia, *Oreochromis niloticus*, and the zebrafish, *Danio rerio*, with the Medium-sensitivity settings in Geneious. This enabled us to identify cone and rod opsin specific reads. If present, paralogous genes were subsequently disentangled following the methods in Musilova et al. (2019a) and de Busserolles et al. (2017). Briefly, we created species-specific references of the expressed opsin genes and their several copies (Musilova et al. 2019a) and remapped the transcriptome reads with medium–low sensitivity to obtain copy-specific expression levels. If multiple opsin genes were found to be expressed, we report their proportional expression in relation to the total opsin gene expression (fig. 1). We used the same pipeline to quantify expression of phototransduction cascade genes in five focal deep-sea species (fig. 2 and table S1), and to search for the expression of the *cyp27c1* gene (table S2).

To analyze key amino-acid substitutions in *RH1 and RH2* and potential shifts in their absorbance, we first translated the opsin coding sequences into amino acid sequences, and then aligned them with the bovine *RH1* (GenBank Acc.No: M12689). We have specifically focused on the positions identified as key-tuning sites in Yokoyama (2008) and Musilova et al. (2019a). For details, see tables 2 and 3. Unfortunately, we were not able to estimate the sensitivity shift of rod opsin copies in *C. warmingii* as only four of the amino acids that were substituted at the 15 key-tuning amino acid sites corresponded with previously tested cases (Yokoyama 2008; Musilova et al. 2019a). Out of the three copies, *RH1-2* has three out of four longer-shifting amino acid variants in these four sites and we assume it is therefore red-shifted. *RH1-1* is most likely sensitive to 488 nm, and *RH1-3*, being the shortest, to 468 nm (fig. 3C).

A data set containing *RH1* opsin gene sequences mined from our newly sequenced transcriptomes and genomes and additional *RH1*s obtained from GenBank (GenBank accession numbers listed in fig. 3), were aligned using the MAFFT (Katoh et al. 2009) plugin as implemented in Geneious, and a phylogenetic tree was subsequently reconstructed using MrBayes version 3.2.1 (Ronquist et al. 2012) (fig. 3A). Trees were produced using the Markov chain Monte Carlo analysis which ran for 1 million generations. Trees were sampled every 100 generations, and the printing frequency was 1,000, discarding the first 25% of trees as burn-in. The evolutionary model chosen was GTR model with gamma-distributed rate variation across sites and a proportion of invariable sites. Posterior probabilities (PP) were calculated to evaluate statistical confidence at each node. We used the same approach with an *RH2*-specific reference data set to reconstruct the phylogenetic relationship between the transcriptome-derived deep-sea *RH2* genes (fig. 3B).

Supplementary Material

Supplementary data are available at *Molecular Biology and Evolution* online.

Acknowledgments

We would like to express our thanks to both scientific and technical crew of the Maria S. Merian and Walther Herwig III research cruises in 2015, 2017, and 2020. In addition, we thank Tina Blancke for help with the sample management, and Veronika Truhlářová for technical support and lab management. We would also like to thank three anonymous reviewers for their comments improving the final version of the manuscript. NL and ZM were supported by the Swiss National Science Foundation (PROMYS-166550), ZM by the PRIMUS Research Programme (Charles University), the Czech Science Foundation (21-31712S) and the Basler Stiftung fuer Experimentelle Zoologie, and FC by an Australian Research Council (ARC) Discovery Early Career Award (DECRA) Fellowship (DE200100620).

Data Availability

Newly sequenced transcriptomes and genomes have been submitted to the SRA database in NCBI under BioProject accession number PRJNA754116. Accession numbers for individual samples are listed in Table 1, and single genes extracted from the transcriptomic and genomic data are available in the Supplementary file 1.

References

Andrews S. 2017. FastQC: a quality control tool for high throughput sequence data. Version 0.11.6. Available from: http://www.bioinformatics.babraham.ac.uk/projects/fastqc

Baylor DA. 1987. Photoreceptor signals and vision. Proctor lecture. *Investigat Ophthalmol Visual Sci*. 28:1.

Betancur RR, Wiley EO, Arratia G, Acero A, Bailly N, Miya M, Lecointre G, Ortí G. 2017. Phylogenetic classification of bony fishes. *BMC Evol Biol*. 17(1):162.

Biagioni LM, Hunt DM, Collin SP. 2016. Morphological characterization and topographic analysis of multiple photoreceptor types in the retinae of mesopelagic hatchetfishes with tubular eyes. *Front Ecol Evol*. 4:25.

Britt LL, Loew ER, McFarland N. 2001. Visual pigments in the early life stages of Pacific northwest marine fishes. *J Exp Biol*. 204(14):2581–2587.

Bowmaker JK, Semo M, Hunt DM, Jeffery G. 2008. Eel visual pigments revisited: the fate of retinal cones during metamorphosis. *Vis Neurosci*. 25(3):249–255.

Bozzano A, Pankhurst PM, Sabatés A. 2007. Early development of eye and retina in lanternfish larvae. *Vis Neurosci*. 24(3):423–436.

Byun J-H, Hyeon J-Y, Kim E-S, Kim B-H, Miyanishi H, Kagawa H, Takeuchi Y, Kim S-J, Takemura A, Hur S-P. 2020. Gene expression patterns of novel visual and non-visual opsin families in immature and mature Japanese eel males. *PeerJ*. 8:e8326.

Carleton KL, Dalton BE, Escobar-Camacho D, Nandamuri SP. 2016. Proximate and ultimate causes of variable visual sensitivities: insights from cichlid fish radiations. *Genesis* 54(6):299–325.

Carleton KL, Escobar-Camacho D, Stieb SM, Cortesi F, Marshall NJ. 2020. Seeing the rainbow: mechanisms underlying spectral sensitivity in teleost fishes. *J Exp Biol*. 223(8):jeb193334.

Collin SP, Hoskins RV, Partridge JC. 1998. Seven retinal specializations in the tubular eye of the *Scopelarchus michaelsarsi*: a case study in visual optimization. *Brain Behav Evol*. 1998(09):291–314.

Collin SP, Marshall NJ. 2003. Sensory processing in aquatic environments. New York: Springer.

Cortesi F, Musilová Z, Stieb SM, Hart NS, Siebeck UE, Malmstrøm M, Tørresen OK, Jentoft S, Cheney KL, Marshall NJ, et al. 2015. Ancestral duplications and highly dynamic opsin gene evolution in percomorph fishes. *Proc Natl Acad Sci U S A*. 112(5):1493–1498.,.

Cortesi F, et al. 2016. From crypsis to mimicry: changes in colour and the configuration of the visual system during ontogenetic habitat transitions in a coral reef fish. *J Exp Biol*. 219(16):2545–2558.

Cortesi F, Mitchell LJ, Tettamanti V, Fogg LG, de Busserolles F, Cheney KL, Marshall NJ. 2020. Visual system diversity in coral reef fishes. *Semin Cell Dev Biol*. 106:31–42.

Cortesi F, et al. 2021. Multiple ancestral duplications of the red-sensitive opsin gene (LWS) in teleost fishes and convergent spectral shifts to green vision in gobies. bioRxiv. doi: 10.1101/2021.05.08.443214.

de Busserolles F, Cortesi F, Helvik JV, Davies WIL, Templin RM, Sullivan RKP, Michell CT, Mountford JK, Collin SP, Irigoien X, et al. 2017. Pushing the limits of photoreception in twilight conditions: the rod-like cone retina of the deep-sea pearlsides. *Sci Adv*. 3(11):eaao4709.

de Busserolles F, Fogg L, Cortesi F, Marshall J. 2020. The exceptional diversity of visual adaptations in deep-sea teleost fishes. *Semin Cell Dev Biol*. 106:20–30.

Dalton BE, Loew ER, Cronin TW, Carleton KL. 2014. Spectral tuning by opsin coexpression in retinal regions that view different parts of the visual field. *Proc R Soc B: Biol Sci*. 281:1797.

Denton EJ. 1990. Light and vision at depths greater than 200 metres. In: Herring PJ, Campbell AK, Whitfield M, Maddock L, editors. Light and life in the sea. Cambridge, UK: Cambridge University Press. p. 127–148.

Denton EJ, Herring PJ, Widder EA, Latz MF, Case JF. 1985. The roles of filters in the photophores of oceanic animals and their relation to vision in the oceanic environment. *Proc R Soc Lond Ser B. Biol Sci*. 225:1238.

Douglas RH, Partridge JC, Marshall NJ. 1998. The visual systems of deep-sea fish. I. Optics, tapeta, visual and lenticular pigmentation. *Prog. Ret. Eye Res*. 17(4):597–636.

Douglas RH, Genner MJ, Hudson AG, Partridge JC, Wagner HJ. 2016. Localisation and origin of the bacteriochlorophyll-derived photosensitizer in the retina of the deep-sea dragon fish *Malacosteus niger*. *Sci Rep*. 6:39395.

Downes GB, Gautam N. 1999. The G protein subunit gene families. *Genomics*. 62(3):544–552. p

Enright JM, Toomey MB, Sato S-y, Temple SE, Allen JR, Fujiwara R, Kramlinger VM, Nagy LD, Johnson KM, Xiao Y, et al. 2015. *Cyp27c1* red-shifts the spectral sensitivity of photoreceptors by converting vitamin A1 into A2. *Curr Biol*. 25(23):3048–3057.

Huang Z, Titus T, Postlethwait JH, Meng F. 2019. Eye degeneration and loss of otx5b expression in the cavefish *Sinocyclocheilus tileihornes*. *J Mol Evol*. 87(7–8):199–208.

Hunt DM, Fitzgibbon J, Slobodyanyuk SJ, Bowmaker JK, Dulai KS. 1997. Molecular evolution of the cottoid fish endemic to Lake Baikal deduced from nuclear DNA evidence. *Mol Phylogenet Evol*. 8(3):415–422.

Hunt DM, Hankins MW, Collin SP, Marshall NJ. 2014. Evolution of visual and non-visual pigments. Vol. 4. Boston (MA): Springer.

Katoh K, Asimenos G, Toh H. 2009. Bioinformatics for DNA sequence analysis multiple alignment of DNA sequences with MAFFT. Totowa (NJ): Humana Press. p. 39–64.

Kawamura S, Tachibanaki S. 2012. Explaining the functional differences of rods versus cones. *Wires Membr Transp Signal*. 1(5):675–683.

Kearse M, Moir R, Wilson A, Stones-Havas S, Cheung M, Sturrock S, Buxton S, Cooper A, Markowitz S, Duran C, et al. 2012. Geneious basic: an integrated and extendable desktop software platform for

the organization and analysis of sequence data. *Bioinformatics*. 28(12):1647–1649.
Kenaley CP, Devaney SC, Fjeran TT. 2014. The complex evolutionary history of seeing red: molecular phylogeny and the evolution of an adaptive visual system in deep-sea dragonfishes (Stomiiformes: Stomiidae). *Evolution* 68(4):996–1013.
La Vail MM, Rapaport DH, Rakic P. 1991. Cytogenesis in the monkey retina. *J Comp Neurol*. 309(1):86–114.
Lamb TD. 2013. Evolution of phototransduction, vertebrate photoreceptors and retina. *Prog Retin Eye Res*. 36:52–119.
Lamb TD. 2019. Evolution of the genes mediating phototransduction in rod and cone photoreceptors. *Prog Retinal Eye Res*. 76:100823.
Larhammar D, Nordström K, Larsson TA. 2009. Evolution of vertebrate rod and cone phototransduction genes. *Phil Trans R Soc B*. 364(1531):2867–2880. p
Liu D-W, Wang F-Y, Lin J-J, Thompson A, Lu Y, Vo D, Yan HY, Zakon H. 2019. The cone opsin repertoire of osteoglossomorph fishes: gene loss in mormyrid electric fish and a long wavelength-sensitive cone opsin that survived 3R. *Mol Biol Evol*. 36(3):447–457.
Lythgoe JN. 1966. In: Rackham O, editor. Light as an ecological factor visual pigments and under – water vision. Oxford: Blackwell.
Luehrmann M, Carleton KL, Cortesi F, Cheney KL, Marshall NJ. 2019. Cardinalfishes (Apogonidae) show visual system adaptations typical of nocturnally and diurnally active fish. *Mol Ecol*. 28(12):3025–3041.
Luo D-G, Silverman D, Frederiksen R, Adhikari R, Cao L-H, Oatis JE, Kono M, Cornwall MC, Yau K-W. 2020. Apo-opsin and its dark constitutive activity across retinal cone subtypes. *Curr Biol*. 30(24):4921–4931.e5.
Mariani AP. 1986. Photoreceptors of the larval tiger salamander retina. *Proc R Soc Lond. Ser B. Biol Sci*. 227:1249.
Mears AJ, Kondo M, Swain PK, Takada Y, Bush RA, Saunders TL, Sieving PA, Swaroop A. 2001. *Nrl* is required for rod photoreceptor development. *Nat Genet*. 29(4):447–452.
Moser HG, Smith PE. 1993. Larval fish assemblages and oceanic boundaries. *Bull Mar Sci*. 53(2):283–289.
Munk O. 1990. Changes in the visual cell layer of the duplex retina during growth of the eye of a deep-sea teleost, *Gempylus serpens* Cuvier, 1829. *Acta Zool*. 71(2):89–95.
Musilova Z, Cortesi F, Matschiner M, Davies WIL, Patel JS, Stieb SM, de Busserolles F, Malmstrøm M, Tørresen OK, Brown CJ, et al. 2019a. Vision using multiple distinct rod opsins in deep-sea fishes. *Science* 364(6440):588–592.
Musilova Z, et al. 2019b. Evolution of the visual sensory system in cichlid fishes from crater lake Barombi Mbo in Cameroon. *Mol Ecol*. 28:5010–5031.
Musilova Z, Salzburger W, Cortesi F. 2021. The visual opsin gene repertoires of teleost fishes: evolution, ecology and function. *Annu Rev Cell Dev Biol*. 37(1). https://doi.org/10.1146/annurev-cellbio-120219-024915.
Musilova Z, Cortesi F. 2021. Multiple ancestral and a plethora of recent gene duplications during the evolution of the green sensitive opsin genes (RH2) in teleost fishes. bioRxiv. doi: 10.1101/2021.05.11.443711.
Partridge JC, Shand J, Archer SN, Lythgoe JN, van Groningen-Luyben WA. 1989. Interspecific variation in the visual pigments of deep-sea fishes. *J Comp Physiol A*. 164(4):513–529.
Partridge JC, Archer SN, van Oostrum J. 1992. Single and multiple visual pigments in deep-sea fishes. *J Mar Biol Ass*. 72(1):113–130.
Pointer MA, Carvalho LS, Cowing JA, Bowmaker JK, Hunt DM. 2007. The visual pigments of a deep-sea teleost, the pearl eye *Scopelarchus analis*. *J Exp Biol*. 210(16):2829–2835.
Raymond PA. 1995. Neurobiology and clinical aspects of the outer retina development and morphological organization of photoreceptors. Dordrecht: Springer. p. 1–23.
Ronquist F, Teslenko M, van der Mark P, Ayres DL, Darling A, Höhna S, Larget B, Liu L, Suchard MA, Huelsenbeck JP, et al. 2012. MrBayes 3.2: efficient Bayesian phylogenetic inference and model choice across a large model space. *Syst Biol*. 61(3):539–542.
Sassa C, Hirota Y. 2013. Seasonal occurrence of mesopelagic fish larvae on the onshore side of the Kuroshio off southern Japan. *Deep Sea Res Part I: Oceanogr Res Papers*. 81:49–61.
Savelli I, Flamarique IN, Iwanicki T, Taylor JS. 2018. Parallel opsin switches in multiple cone types of the starry flounder retina: tuning visual pigment composition for a demersal life style. *Sci Rep*. 8(1):1.
Schott RK, Bhattacharyya N, Chang BS. 2019. Evolutionary signatures of photoreceptor transmutation in geckos reveal potential adaptation and convergence with snakes. *Evolution* 73(9):1958–1971.
Sernagor E, Eglen S, Harris B, Wong R. 2006. Retinal development. New York (NY): Cambridge University Press.
Shen YC, Raymond PA. 2004. Zebrafish cone-rod (*crx*) homeobox gene promotes retinogenesis. *Dev Biol*. 269(1):237–251.
Simoes BF, et al. 2016. Multiple rod–cone and cone–rod photoreceptor transmutations in snakes: evidence from visual opsin gene expression. *Proc R Soc B: Biol Sci*. 283(1823):20152624.
Stieb SM, de Busserolles F, Carleton KL, Cortesi F, Chung W-S, Dalton BE, Hammond LA, Marshall NJ. 2019. A detailed investigation of the visual system and visual ecology of the Barrier Reef anemonefish, *Amphiprion akindynos*. *Sci Rep*. 9(1):1.
Sugawara T, Terai Y, Imai H, Turner GF, Koblmuller S, Sturmbauer C, Shichida Y, Okada N. 2005. Parallelism of amino acid changes at the RH1 affecting spectral sensitivity among deep-water cichlids from Lakes Tanganyika and Malawi. *Proc Natl Acad Sci U S A*. 102(15):5448–5453.
Tettamanti V, de Busserolles F, Lecchini D, Marshall NJ, Cortesi F. 2019. Visual system development of the spotted unicornfish, *Naso brevirostris* (Acanthuridae). *J. Exp. Biol*. 222(24):jeb209916.
Torres-Dowdall J, Pierotti MER, Härer A, Karagic N, Woltering JM, Henning F, Elmer KR, Meyer A. 2017. Rapid and parallel adaptive evolution of the visual system of Neotropical Midas cichlid fishes. *Mol Biol Evol*. 34(10):2469–2485.
Turner JR, White EM, Collins MA, Partridge JC, Douglas RH. 2009. Vision in lanternfish (Myctophidae): adaptations for viewing bioluminescence in the deep-sea. *Deep Sea Res Part I: Oceanogr Res Papers*. 56(6):1003–1017.
Valen R, Eilertsen M, Edvardsen RB, Furmanek T, Rønnestad I, van der Meeren T, Karlsen Ø, Nilsen TO, Helvik JV. 2016. The two-step development of a duplex retina involves distinct events of cone and rod neurogenesis and differentiation. *Dev Biol*. 416(2):389–401.
Wagner HJ, Partridge JC, Douglas RH. 2019. Observations on the retina and 'optical fold'of a mesopelagic sabretooth fish, *Evermanella balbo*. *Cell Tissue Res*. 378(3):411–425.
Yokoyama S. 2008. Evolution of dim-light and color vision pigments. *Annu Rev Genomics Hum Genet*. 9:259–282.
Yokoyama S, Jia H. 2020. Origin and adaptation of green-sensitive (RH2) pigments in vertebrates. *FEBS Open Bio*. 10(5):873–882.
Zhang H, Futami K, Horie N, Okamura A, Utoh T, Mikawa N, Yamada Y, Tanaka S, Okamoto N. 2000. Molecular cloning of fresh water and deep-sea rod opsin genes from Japanese eel *Anguilla japonica* and expressional analyses during sexual maturation. *FEBS Lett*. 469(1):39–43.